https://doi.org/10.5194/gmd-2020-269
Preprint. Discussion started: 21 October 2020

Geoscientific Model Development Discussions

ICONGETM v1.0 – Flexible two-way coupling via exchange grids between the unstructured-grid atmospheric model ICON and the structured-grid coastal ocean model GETM

Tobias Peter Bauer[1,2], Knut Klingbeil[2], Peter Holtermann[2], Bernd Heinold[1], Hagen Radtke[2], and Oswald Knoth[1]

[1]Leibniz Institute for Tropospheric Research (TROPOS), Permoserstraße 15, 04318 Leipzig
[2]Leibniz Institute for Baltic Sea Research Warnemünde (IOW), Seestraße 15, 18119 Rostock

Correspondence: Tobias Peter Bauer (tobias.bauer@tropos.de)

Abstract. Coupled atmosphere-ocean models are developed for process understanding at the air-sea interface. Over the last 20 years, there have been studies involving simulations in the range of sub-annual simulations to climate scenarios. The development of coupled models highly depends on the kind and quality of the required data exchange between the model interfaces. This work achieved the development of a two-way coupled atmosphere-ocean model ICONGETM with flexible data exchange via exchange grids provided by the widely used ESMF regridding package. The regridding of flux data between the unstructured atmosphere model ICON and the structured regional ocean model GETM is conducted via these exchange grids. The newly developed model ICONGETM has been demonstrated for a coastal upwelling scenario in the Central Baltic Sea.

1 Introduction

Regional coupled climate models are widely used today, especially for estimating regional impacts of global climate change. The first applications of this method date back to the late 1980s. In the work by Dickinson et al. (1989), a global climate simulation on a $500\,\mathrm{km}$ grid was downscaled to a $60\,\mathrm{km}$ grid over the Western United States, using land-atmosphere coupling. This application of local-area models was computationally limited to few years of simulation at that time, and only when the computational power increased such models could be run over decadal periods and were called regional climate models (RCMs, Laprise, 2008). In early applications, they were used as a link between general circulation models which provided climate information and localized components like hydrology models which required this input on a finer spatial scale (e.g. Miller and Kim, 1996). A widespread use of regional climate modelling started in the late 1990s because global climate models showed unacceptable biases in the areas of interest (Schrum, 2017). First climate downscalings were done with uncoupled models, later the coupled atmosphere-ocean strategy of the global models has also been used in downscaling applications (e.g. Aldrian et al., 2005; Ren and Qian, 2005; Seo et al., 2007). For most atmospheric quantities of interest like precipitation over land, however, the ocean-atmosphere coupling in the regional setup is not always required, since atmospheric circulation and moisture fluxes, e.g. by precipitation over sea, are driven on larger spatial scales. On the other hand, when climate effects on

https://doi.org/10.5194/gmd-2020-269
Preprint. Discussion started: 21 October 2020


Geoscientific Model Development Discussions

the regional ocean are of interest, the application of regional ocean models is crucial since e.g. coastal dynamics intrinsically have smaller spatial scales than atmospheric circulation.

For the Baltic Sea area, coupled models are applied for more than 20 years. Earlier studies were limited by computational resources, either to sub-annual runs (e.g. Gustafsson et al., 1998) or to models without a 3-dimensional ocean representation (e.g. Rummukainen et al., 2001). Model experiments were conducted with the aims of improving weather predictions or process understanding of air-sea interactions (e.g. Schrum et al., 2003).

Present-day applications of coupled model systems include downscaling experiments of climate scenarios (e.g., Christensen et al., 2019; Gröger et al., 2019), with resolutions down to $0.11°$ in the atmosphere and two nautical miles in the ocean for multi-decadal runs. A next step will be the application of convection-permitting models which show an atmospheric horizontal resolution around $2\,\mathrm{km}$, which allows for the representation of convective processes in the troposphere and for a more accurate representation of extreme rainfall events (Clark et al., 2016; Purr et al., 2019). A high resolution in ocean models is required to resolve certain baroclinic structures like mesoscale or submesoscale eddies or coastally trapped waves. The latter e.g. determine the spatial structure of coastal upwelling cells. They are confined to the near-coastal area, with a characteristic length scale of the baroclinic Rossby radius, $1.3 - 7\,\mathrm{km}$ in the Baltic Sea (Fennel et al., 1991), and the failure to resolve them may lead to an unrealistic representation of upwelling cells and filaments (Fennel et al., 2010). Resolving filaments of eddies is important both from a physical and biogeochemical point of view, since they induce horizontal mixing (Badin et al., 2011) as well as provide spatial heterogeneity that may support primary production due to non-linear interactions (Woodward et al., 2019).

A key element of coupled atmosphere-ocean models is the data exchange at the air-sea interface and the treatment of the different coastline representations in each model grid. The development of coupled atmosphere-ocean models is nowadays based on software libraries which provide a set of tools for communication, interpolation and data exchange between different model components. Most prominent examples are ESMF (Hill et al., 2004; Theurich et al., 2016) and OASIS (Valcke, 2013). Especially the Earth System Modelling Framework (ESMF) supports a general application with different horizontal meshes, conservative interpolation, automated driving of coupled processes as well as model controlled data handling. The data transfer via an exchange grid (Balaji et al., 2006) allows the implementation of an algorithm which automatically detects the coastline representation and a conservative interpolation between model components. Another main feature of ESMF is the National Unified Operational Prediction Capability (NUOPC) layer, which aims at standardized infrastructure for model interaction (Theurich et al., 2016).

This paper describes the newly developed coupled atmosphere-ocean modelling system ICONGETM based on ESMF. The system consists of the next-generation atmosphere model ICON (Zängl et al., 2015) and the regional ocean model GETM (Burchard and Bolding, 2002). It provides conservative flux exchange for different coastline representations and a model-controlled data handling. First, the technical structure of ICONGETM including a short overview of ICON and GETM as well as the automated data exchange is described in Sec. 2. In Sec. 3, the data transfer and interpolation using the ESMF exchange grid is explained. Finally, an application of the coupled model system to the Central Baltic Sea is presented in Sec. 4.

https://doi.org/10.5194/gmd-2020-269
Preprint. Discussion started: 21 October 2020


Geoscientific Model Development Discussions

2 The coupled model system ICONGETM

2.1 The atmospheric model ICON

The ICOsahedral Non-hydrostatic modeling framework (ICON) was developed by the German Weather Service (DWD) and the Max Planck Institute for Meteorology (MPI-M) as a unified modelling system for global numerical weather prediction (NWP) and climate modelling, including exact local mass conservation, mass-consistent tracer transport, a flexible grid nesting capability and the usage of nonhydrostatic Euler equations on global domains (e.g. Dipankar et al., 2015; Zängl et al., 2015; Heinze et al., 2017; Giorgetta et al., 2018; Crueger et al., 2018; Borchert et al., 2018). The details of the model are given in Zängl et al. (2015). They have been summarized in Ullrich et al. (2017) for the dynamical core model inter-comparison project (DCMIP) 2016.

ICON solves the 2-D vector-invariant equations on an icosahedral (triangular) grid with Arakawa C-grid staggering and terrain-following vertical discretization. A predictor–corrector scheme is employed, which is explicit in all terms except for those describing the vertical propagation of sound waves. The physic parameterization is based on the physics from the COSMO model, see Doms et al. (2011); Zängl et al. (2015). The nesting capability in ICON includes a bisection of the simulation time step from one nest to the other.

The DWD applies ICON as a member of the operative weather forecast system in Germany (DWD, 2019). High-resolutions simulations were conducted to understand the physical feedbacks due to clouds (e.g. Dipankar et al., 2015; Heinze et al., 2017). MPI-M uses the ICON Earth system model (ICON-ESM; e.g. Hanke et al., 2016; Giorgetta et al., 2018; Crueger et al., 2018), where individual model components for the atmosphere (ICON-A), ocean (ICON-O) and land (ICON-L) are coupled with the YAC library (Hanke et al., 2016).

For coupling in ICONGETM an interface to ESMF was implemented for the nonhydrostatic NWP core.

2.2 The ocean model GETM

The General Estuarine Transport Model (GETM) is an open-source ocean model for coastal and regional applications (www.getm.eu). Originally developed for solving the primitive equations as well as transport equations for temperature and salinity on C-staggered finite volumes (Burchard and Bolding, 2002), it nowadays also offers a non-hydrostatic extension of the dynamic kernel (Klingbeil and Burchard, 2013). GETM supports boundary-following vertical coordinates with adaptive interior model layers (Hofmeister et al., 2010; Gräwe et al., 2015). The nonlinear free surface is computed by a split-explicit mode-splitting technique with drying-and-flooding capability (see the review about numerics of coastal ocean models by Klingbeil et al., 2018). GETM uses efficient 2nd-order transport schemes with minimized spurious mixing (Klingbeil et al., 2014). State-of-the-art turbulence closure is provided from the General Ocean Turbulence Model (GOTM; www.gotm.net). Via an interface to the Framework for Aquatic Biogeochemical Models (FABM; www.fabm.net) GETM can act as a hydrodynamic host model for a variety of biogeochemical models. An efficient decomposition into subdomains offers high-performance computing on massively parallel systems for high-resolution and climate-scale simulations (e.g. Lange et al., 2020; Gräwe et al., 2019). For coupling to other models GETM already provides an interface to ESMF (Lemmen et al., 2018).

https://doi.org/10.5194/gmd-2020-269
Preprint. Discussion started: 21 October 2020

Geoscientific Model Development Discussions
Open Access
EGU

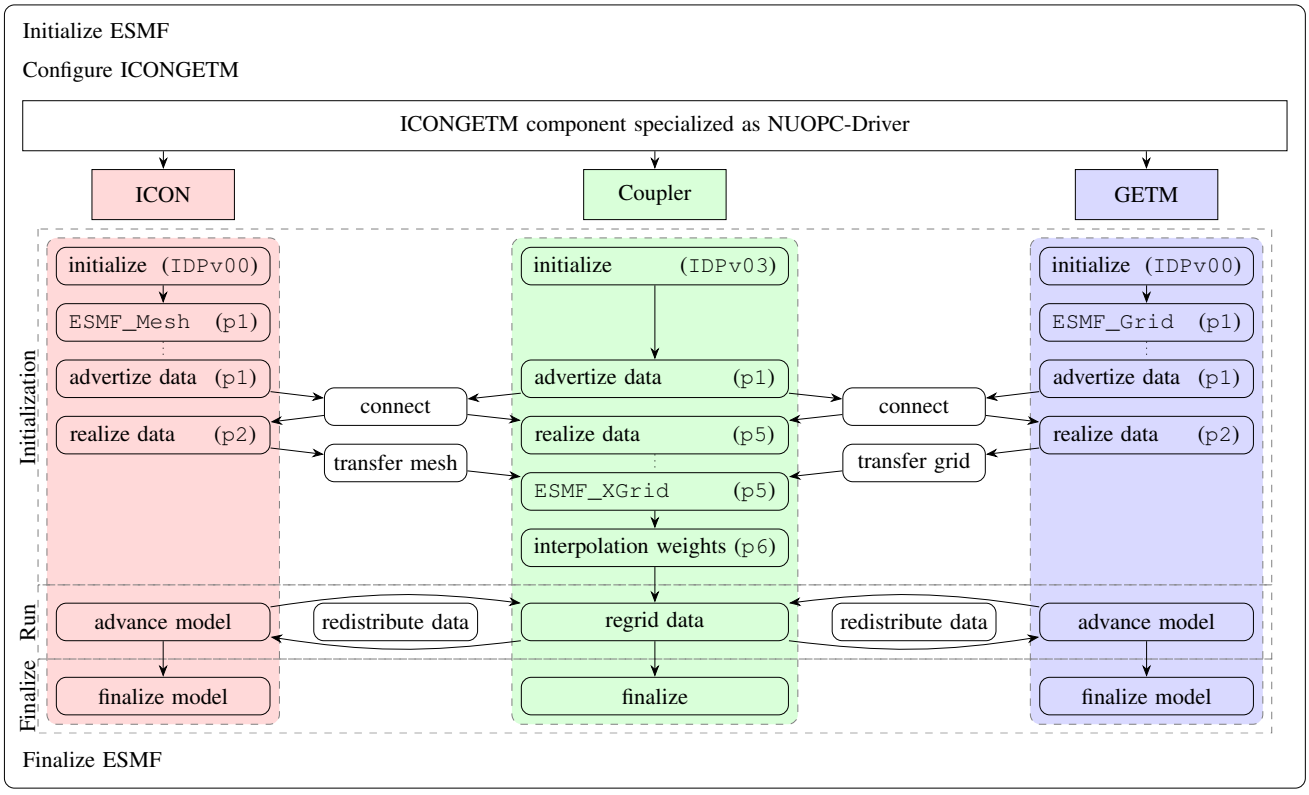

Figure 1. Structure of ICONGETM. The ICONGETM component created by the main program is specialized as NUOPC-Driver and consists of NUOPC-Model components for ICON and GETM as well as a NUOPC-Mediator for the Coupler. For all components the implemented specialized routines for initialization, run and finalization are indicated. The initialization phases of the NUOPC-layer are given in parenthesis. Automated generic NUOPC operations are represented by arrows.

2.3 Coupling with ESMF/NUOPC

ICONGETM is built on ESMF/NUOPC. It is hierarchically structured into main program, driver, model and coupler components (see Fig. 1). The Earth System Modelling Framework (ESMF) library contains superstructure features for representing model and coupler components as well as infrastructure features, including grid remapping, time management, model documentation, and data communications, see Theurich et al. (2016). The NUOPC-layer controls the execution and interaction of the model and coupler components by triggering different phases for their Initialization, Run and Finalization. Generic actions are performed automatically and for the model and coupler components only individual specification routines need to be implemented.

https://doi.org/10.5194/gmd-2020-269
Preprint. Discussion started: 21 October 2020

Geoscientific Model Development Discussions
Open Access
EGU

Quantity	ICON		Coupler	GETM		one-/two-way
sea surface temperature	t_seasfc	[K]	⟸	T(:,:,kmax)	[°C]	(2w)
mean sea level air pressure	pres_msl	[Pa]	⟹	slp	[Pa]	(1w, 2w)
gridscale rain rate	rain_gsp_rate	$[\mathrm{kg\,m^{-2}s^{-1}}]$				
gridscale snow rate	snow_gsp_rate	$[\mathrm{kg\,m^{-2}s^{-1}}]$	⟹	precip	$[\mathrm{ms^{-1}}]$	(1w, 2w)
convective rain rate	rain_con_rate	$[\mathrm{kg\,m^{-2}s^{-1}}]$				
convective snow rate	snow_con_rate	$[\mathrm{kg\,m^{-2}s^{-1}}]$				
surface moisture flux	qhfl_s	$[\mathrm{kg\,m^{-2}s^{-1}}]$	⟹	evap	$[\mathrm{ms^{-1}}]$	(1w, 2w)
u-momentum flux at surface	umfl_s	$[\mathrm{N\,m^{-2}}]$	⟹ (R)	tausx	$[\mathrm{N\,m^{-2}}]$	(1w, 2w)
v-momentum flux at surface	vmfl_s	$[\mathrm{N\,m^{-2}}]$	⟹ (R)	tausy	$[\mathrm{N\,m^{-2}}]$	(1w, 2w)
surface sensible heat flux	shfl_s	$[\mathrm{W\,m^{-2}}]$				
surface latent heat flux	lhfl_s	$[\mathrm{W\,m^{-2}}]$	⟹	shf	$[\mathrm{W\,m^{-2}}]$	(1w, 2w)
longwave net flux at surface	thb_s	$[\mathrm{W\,m^{-2}}]$				
shortwave net flux at surface	sob_s	$[\mathrm{W\,m^{-2}}]$	⟹	swr	$[\mathrm{W\,m^{-2}}]$	(1w, 2w)
zonal wind in 10 m	u_10m	$[\mathrm{ms^{-1}}]$	⟹ (R)	u10	$[\mathrm{ms^{-1}}]$	
meridional wind in 10 m	v_10m	$[\mathrm{ms^{-1}}]$	⟹ (R)	v10	$[\mathrm{ms^{-1}}]$	
temperature in 2 m	t_2m	[K]	⟹	t2	[K]	
dew point in 2 m	td_2m	[K]	⟹	hum	[K]	
relative humidity in 2 m	rh_2m	$[1 \times 10^{-2}]$	⟹	hum	$[1 \times 10^{-2}]$	
total cloud cover	clct	[1]	⟹	tcc	[1]	

Table 1. List of quantities which can be exchanged in ICONGETM. The direction is indicated by the arrow. The units of the source and target variables are given in square brackets. Data conversion and aggregation is done in the coupler. `precip` and `evap` are obtained by division with the reference density of fresh water. If graupel, ice and hail are activated in ICON, then the corresponding contributions to precipitation must also be considered. Wind data need to be rotated (R) to the local coordinate system in GETM. The humidity quantity is correctly identified by the name of the exchanged ESMF field. The exchange of flux data (3rd block) or state variables (last block) offers the comparison of different coupling strategies within the same model environment. The last column indicates which data are exchanged during the performed one- and two-way coupled simulations.

2.3.1 Initialization

ICONGETM is initialized and configured in different stages. At first, ESMF itself is initialized. Next, the coupled model is configured from a user-provided configuration file with the number of processes for each model component, the names of the data to be received by each model component as well as the coupling time step.

A NUOPC-Driver is applied, which creates NUOPC-Model components for ICON and GETM as well as a NUOPC-Mediator, which serves as a data exchange component between the model components. The current implementation only

https://doi.org/10.5194/gmd-2020-269
Preprint. Discussion started: 21 October 2020


Geoscientific Model Development Discussions

supports a concurrent distribution of the components among all available computing units. For the time management, a run sequence defines in which order the mediator and model components will interact during the simulation.

Next, the initialization routines of each NUOPC-Model component are called. They have access to the initializing routines of the individual models themselves. Additionally, the horizontal grid structures are translated into an `ESMF_Grid` and `ESMF_Mesh` for structured and unstructured discretizations, respectively, see Sec. 3.1 and 3.2. Moreover, `ESMF_Fields` are created to advertise all data which are available for exchange. However, based on the user-specified lists of data that should be received by each model component, the model system automatically detects the required subset of fields which are finally connected and realized. The current implementation supports the exchange of flux and state data, see Tab. 1 for a list of exchangeable quantities and their optional conversion by the mediator.

The data transfer between the NUOPC-Models via the NUOPC-Mediator is then prepared generically, i.e. by the NUOPC layer. NUOPC-Connectors are set up to redistribute the data between the different computing units used by the coupler and model components. For the actual regridding (interpolation) between the horizontal triangular grid from ICON and the horizontal latitude-longitude grid from GETM, one `ESMF_XGrid` is created for each direction. For details see Sec. 3. The interpolation weights are calculated only once during initialization and will be used in the Run phase. The generation of the `ESMF_XGrid` and the interpolation weights is the most expensive part of the overall overhead due to coupling. The later performed interpolation in the Run phase is relatively cheap.

In the present implementation, no model receives data during Initialization phase. However, the first data exchange takes place at the beginning of the Run phase, as specified in the run sequence. All model components update their export fields at the end of the Initialization phase.

2.3.2 Run

During runtime the coupled model system is integrated in time by repeating the prescribed run sequence with the given coupling intervals until the simulation end time is reached. At the beginning of the run sequence new input data are provided to each model component by data exchange and regridding via the mediator component. In ICON, the received data must be copied to model internal memory locations. For GETM, the `ESMF_Fields` already contain pointers to the internal memory. With the new data from the import fields each model advances with its own time step until the next coupling time point is reached. At the end of the run sequence all model components prepare the following data exchange by updating their export fields from the internal model memory.

2.3.3 Finalization

This phase finalizes all ESMF and NUOPC components. The finalization of the model compoents is included by calling the finalizing interface in ICON and GETM. The overall last step is the finalization of ESMF.

https://doi.org/10.5194/gmd-2020-269
Preprint. Discussion started: 21 October 2020


Geoscientific Model Development Discussions

3 Data exchange between ICON and GETM

The data exchange between ICON and GETM is based on the regridding from the source model grid to an exchange grid and the regridding from the exchange grid to the target model grid. The ESMF exchange grid (`ESMF_XGrid`) infrastructure is used for the conservative interpolation at the air-sea interface, i.e. in the NUOPC-Mediator, compare with Fig. 1. The aim is to apply an interpolation approach which is independent of any horizontal resolution in ICON and GETM. Before the `ESMF_XGrid` and how it is utilized in ICONGETM is explained in detail, the horizontal discretization of ICON and GETM is presented. Furthermore, the interpolation is schematically described.

3.1 Triangular mesh in ICON

The horizontal grid structure of ICON is described in detail by Linardakis et al. (2011). The very first assumption for the horizontal grid is that the Earth is approximated as a sphere. It is based on the projection of an icosahedron onto the sphere. The edges of each triangle of the icosahedron can now be interpreted as an arc of great circles on the sphere. A refinement of the grid, i.e. to increase the resolution by using smaller triangles, is achieved by a combination of two steps. The first step is an initial division of the original icosahedron triangle edges by $n \in \mathbb{N}$. The second step are $k \in \mathbb{N}$ bisections of the remaining smaller triangles. The final grid is then described by RnBk. The number of triangles on the sphere for a grid RnBk is given by $20n^2 4^k$, see Zängl et al. (2015). The effective grid resolution is given by

$$\sqrt{\frac{\pi}{5}} \frac{r_{\mathrm{E}}}{n2^k} \tag{1}$$

with Earth radius r_{E}. Table 1 in Zängl et al. (2015) shows different R2Bk grids with effective grid resolutions. The DWD applies a global R3B07 grid, a R3B08 Europe-grid and a R3B09 Germany-grid for the weather forecast simulations, which have effective resolutions of $13.15\,\mathrm{km}$, $6.58\,\mathrm{km}$ and $3.29\,\mathrm{km}$, respectively.

The construction of refined grids supports a straight-forward nesting. An example for the Baltic Sea region based on R2B08, R2B09 and R2B10 grids with effective resolutions of $9.89\,\mathrm{km}$, $4.93\,\mathrm{km}$ and $2.47\,\mathrm{km}$ is shown in Fig. 2.

Fig. 3 shows the R2B10 grid over the Island of Gotland in the Central Baltic Sea. Based on various external datasets (e.g. Reinert et al., 2020) every grid cell is associated with a set of fraction values for different land classifications (e.g. forest, urban areas and others). Cells with less than $50\,\%$ of land fraction are considered as water cells. The triangular grid and the associated cell classification are stored in an `ESMF_Mesh` object, which also contains information about the domain decomposition onto computing units. The creation of the `ESMF_Mesh` is computing unit specific. Therefore, the domain distributing among the available computing units performed by ICON is kept in the `ESMF_Mesh` in ICONGETM.

3.2 Structured grid in GETM

The grid in GETM is structured and supports curvilinear horizontal coordinates in Cartesian and latitude-longitude space. For coupling with ICON only grids in spherical coordinates can be used. A land mask defines land and water cells, see

https://doi.org/10.5194/gmd-2020-269
Preprint. Discussion started: 21 October 2020

Geoscientific Model Development Discussions
Open Access
EGU

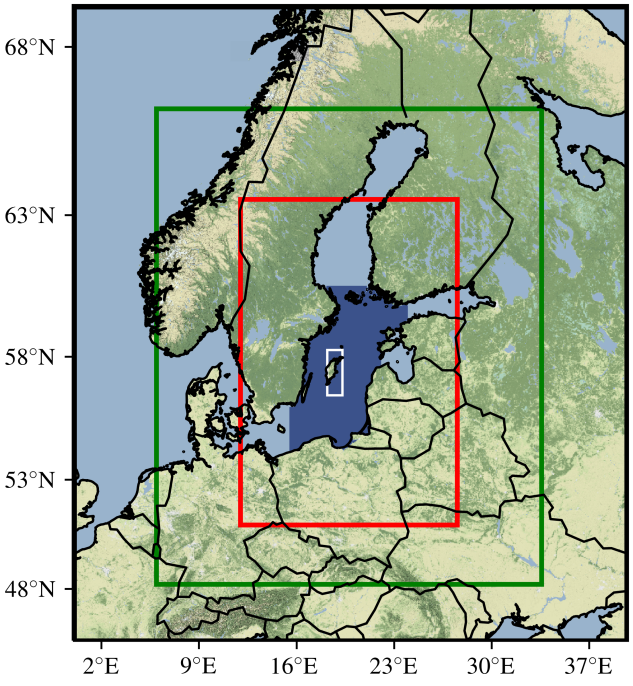

Figure 2. Nesting of different ICON domains with effective resolutions of 9.89 km (black frame), 4.93 km (green frame) and 2.47 km (red frame) over the Baltic Sea region. The darkblue area in the Central Baltic Sea represents the model domain of GETM. The white rectangle frames the area shown in Fig. 3.

Fig. 3. Coordinate, area (defined based on rhumb lines) and mask data as well as information about the domain distribution on computing units are stored in an `ESMF_Grid` object.

3.3 Exchange grid in the coupler

Based on the information provided by the mesh from ICON and the grid from GETM, an exchange grid is created in the coupler. The ESMF library constructs the exchange grid by overlaying both meshes (see Fig. 4), calculation of the intersection points and a final triangulation of all elements, for a schematic representation see Fig. 5. The `ESMF_XGrid` object only consists of elements that are required for the data exchange between the ocean cells in ICON and GETM.

As indicated in Figs. 4 and 5, the overlay of the different grids yields four possible combinations of land/ocean masks:

1. land cells in ICON and GETM,
2. ocean cell in ICON and land cell in GETM,
3. land cell in ICON and ocean cell in GETM,

https://doi.org/10.5194/gmd-2020-269
Preprint. Discussion started: 21 October 2020

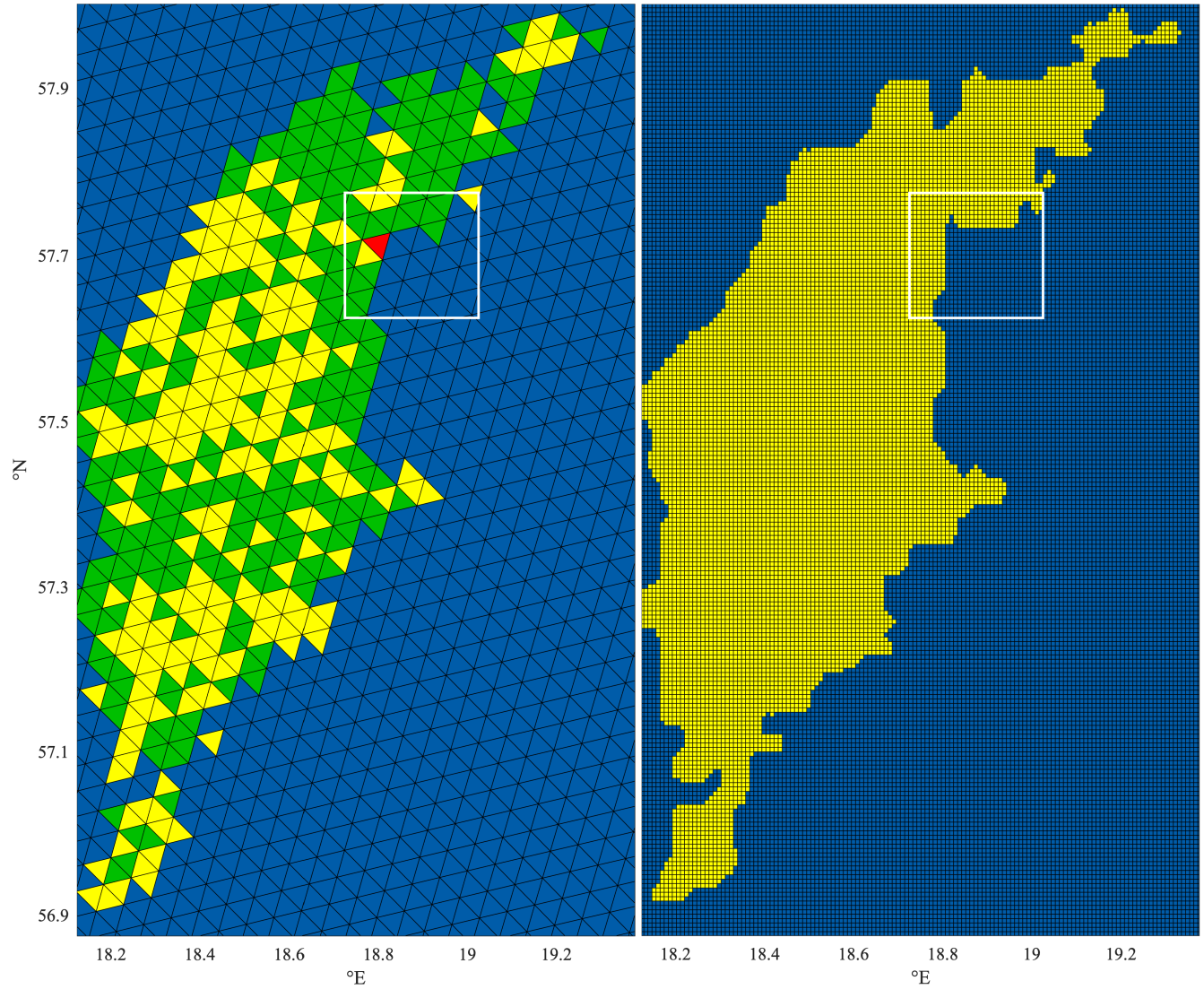

Figure 3. Triangular grid with an effective resolution of 2.47 km used in ICON (left) and rectangular grid with a resolution of approximately 600 m used in GETM (right) over the Island of Gotland in the Central Baltic Sea (see Fig. 2). In the ICON grid, the different colouring represents cells that consist of more than 50% of ocean (blue), forest (green), urban areas (red) or non-specific land classifications (yellow). GETM only distinguishes between ocean (blue) and land (yellow). The white rectangles frame the area shown in Fig. 4.

4. ocean cells in ICON and GETM.

Elements of case 1 and 2 are excluded from the exchange grid, while elements of case 4 are included. Whether the elements of case 3 belong to the exchange grid depends on the direction of interpolation. Therefore, two different exchange grids are

https://doi.org/10.5194/gmd-2020-269
Preprint. Discussion started: 21 October 2020

Geoscientific Model Development
Discussions
Open Access
EGU

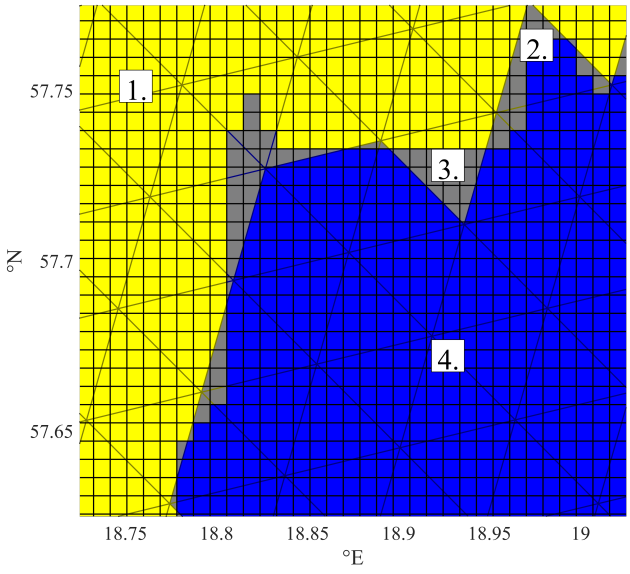

Figure 4. Overlay of the triangular ICON grid and the rectangular GETM grid at the eastern coast of the Island of Gotland in the Central Baltic Sea (see Fig. 3). The four possible combinations of land/ocean masks are labeled. Gray areas mark different land/ocean masks: ICON ocean and GETM land (case 2), ICON land and GETM ocean (case 3).

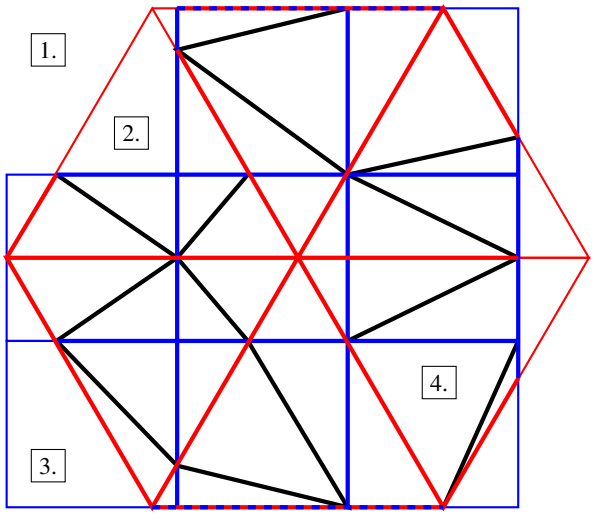

Figure 5. Exemplary 2D exchange grid formed by a triangular atmosphere (red) and a rectangular ocean (blue) grid. The exchange grid consists of edges from the original triangular and rectangular grids (thick red and blue) and additional edges from the triangulation (black). Assuming that only water cells are shown, the four possible combinations of land/ocean masks are labeled. Here the exchange grid is shown for the interpolation from the ocean to the atmosphere grid, therefore, excluding the elements of case 3.

https://doi.org/10.5194/gmd-2020-269
Preprint. Discussion started: 21 October 2020

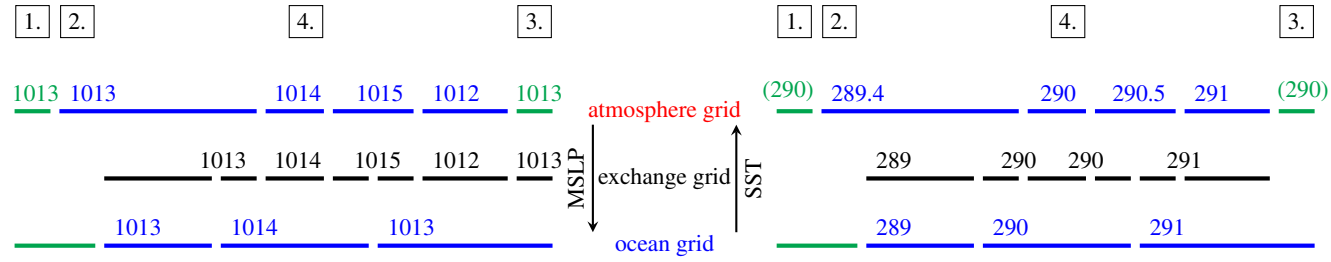

Figure 6. Schematic representation of the regridding between ICON and GETM. In the atmosphere and ocean grids active ocean cells are coloured in blue and land cells in green. As shown for the transfer of mean sea level pressure (MSLP in hPa) and sea surface temperature (SST in K), the exchange grid can consist of different cells for each direction. The four possible combinations of land/ocean masks are indicated. On land (cases 1 and 3) an ICON-internal SST (here 290 K) is used. This ICON-internal SST is also considered for fractions of ocean cells not covered by GETM ocean cells (case 2).

created and used: one for the interpolation from ICON to GETM, which includes the elements of case 3, and one vice versa, excluding elements of case 3, see Fig. 6.

3.4 Regridding

The `ESMF_XGrid` class supports first and second order conservative interpolation. Currently, only the first order method has been applied in ICONGETM. The interpolation weights are calculated during the initialization, based on the areas of the grid cells. The connecting edges between the vertices in the exchange grid are defined on arcs of great circles, which differ from the rhumb lines used in GETM. However, the interpolation between GETM and the exchange grid is still conservative, because the weights are scaled in terms of the area provided by GETM.

3.4.1 Regridding from ICON to GETM

As sketched in Fig. 6 for the regridding of the mean sea level pressure (MSLP), the interpolation from ICON to GETM is straight-forward, because ICON provides all quantities over the whole domain. However, there is a physically inconsistent treatment of surface fluxes calculated over land cells in ICON (thus based on the corresponding parameterizations for land surfaces), but provided to ocean cells in GETM (case 3).

3.4.2 Regridding from GETM to ICON

Fig. 6 sketches the regridding of the sea surface temperature (SST). The update of an ICON ocean cell that is partly covered by a GETM land cell (case 2) needs some remarks. For the contribution from a GETM land cell to an ICON ocean cell, the SST value of the ICON cell is applied. This value can be either a user-provided ICON-internal SST (if the climatological update is activated) or simply the SST from the last time step. For the first time step this is the initial ICON-internal SST.

https://doi.org/10.5194/gmd-2020-269
Preprint. Discussion started: 21 October 2020


Geoscientific Model Development Discussions
Open Access
EGU

4 Demonstration

For demonstration purposes, the newly developed model system ICONGETM is applied to the Central Baltic Sea. High-resolution uncoupled, one-way and two-way coupled simulations are carried out and compared. The modelling period July 1 – 21, 2012 is chosen to evaluate the model results with measurement data from a field campaign with research vessel (RV) Meteor (cruise M87).

4.1 Coupled Central Baltic Sea setup

4.1.1 ICON configuration

ICON is run in limited area mode with three nested domains with effective resolutions of $9.89\,\mathrm{km}$, $4.93\,\mathrm{km}$ and $2.47\,\mathrm{km}$, respectively (see Fig. 2). The vertical terrain-following hybrid grids based on 90, 65 and 54 pressure levels, respectively, are used (Reinert et al., 2020). At the open boundaries the outermost domain is driven by 6-hourly IFS data from ECMWF. The designed nesting guarantees a smooth transition from this coarse boundary forcing (provided with $16\,\mathrm{km}$ resolution) to the innermost domain over the Central Baltic Sea. The feedback from refined nesting levels is relaxation-based. The model time steps are $60\,\mathrm{s}$, $30\,\mathrm{s}$ and $15\,\mathrm{s}$, respectively. For all domains initial conditions are obtained by interpolation from IFS data. In contrast to long term hindcast applications, ICON is not re-initialized during the model run. Within this "free run" the ICON-internal sea surface temperature, prescribed by the OSTIA data from the German Weather Service (Donlon et al., 2012) with a resolution of $\frac{1}{20}^\circ$ (approx. $5\,\mathrm{km}$), is not updated by daily or monthly climatological increments. Apart from that, ICON is configured with similar settings as the DWD uses for the operational weather forecast, i.e. non-hydrostatic numerical weather prediction. These settings include the sub-grid scale cloud scheme as well as the vertical diffusion and transfer turbulent coefficients from COSMO. For the performed summer simulations COSMO microphysics (Bechtold et al., 2008; Zängl et al., 2015) with only two frozen water substances (cloud ice and snow) are applied. The Rapid Radiation Transfer Model (RRTM) of Mlawer et al. (1997) is used. The convection parameterization is switched off for the finest resolved domain. The complete configuration can be found in the code. The run scripts include the namelist settings. A detailed description of the namelist options are provided through the ICON documentation which is part of the ICON model code.

ICON does not need any specific settings when run two-way coupled in ICONGETM, because the coupler will simply overwrite the ICON-internal sea surface temperature with the data provided from GETM.

4.1.2 GETM configuration

The GETM setup for the Central Baltic Sea is taken from Holtermann et al. (2014). The model domain is shown in Fig. 2. Based on an equidistant spherical grid, the horizontal resolution varies between $500\,\mathrm{m}$ and $600\,\mathrm{m}$. In the vertical 100 terrain-following layers with adaptive zooming towards stratification are applied. At the open boundaries hourly data for temperature, salinity, sea surface elevation and normal depth-averaged velocity from the Baltic Sea setup of Gräwe et al. (2019) are prescribed. Furthermore, the freshwater discharge of the five major rivers entering the model domain is prescribed; see Chrysagi et al.

https://doi.org/10.5194/gmd-2020-269
Preprint. Discussion started: 21 October 2020


Geoscientific Model Development Discussions

(2020) for details. The initial temperature and salinity distribution for the present study was obtained by continuing the original simulations of Holtermann et al. (2014) and subsequent distance-weighted nudging with available measurements from the HELCOM database (www.helcom.fi) below $50\,\mathrm{m}$ depths. The 3D model time step is $45\,\mathrm{s}$.

During a spin-up period from 20 May – 30 June 2012 GETM is run uncoupled. In the GETM configuration file two namelist parameters have to be changed for the uncoupled and coupled simulations. The first one specifies whether atmospheric data should be read from file or whether an external coupler will take care of the data provision. A second one specifies whether GETM needs to compute the air-sea fluxes during runtime or whether air-sea fluxes are already provided. In the uncoupled simulation GETM calculates the air-sea fluxes according to the bulk parameterization of Kondo (1975) in terms of hourly meteorological CFSv2 data (Saha et al., 2014) read from file. During the one- and two-way coupled simulations the coupler will provide the air-sea fluxes from ICON.

4.1.3 ICONGETM configuration

The exchanged data for the one- and two-way coupled simulations are listed in Tab. 1. The coupling time step is set to three minutes. For the present setup a good concurrent load-balancing is obtained with 864 processes for ICON and 384 processes for GETM.

4.2 Results

4.2.1 Effects of interactive coupling on meteorology

In the uncoupled and one-way coupled simulations ICON uses its prescribed internal sea surface temperature (SST), which does not show any pronounced temperature gradients due to oceanic eddies or coastal upwelling. Short-term and small-scale variations are only considered in the two-way coupled ICONGETM run (see Fig. 7), with the SST simulated and provided in high-resolution by GETM.

In July 2012, the simulated SST ranged around $289\,\mathrm{K}$, with values below $282\,\mathrm{K}$ in the upwelling areas south of the coast of mainland Sweden and the islands of Öland and Gotland. The ICON-internal SST is between $0.5\,\mathrm{K}$ and $2\,\mathrm{K}$ colder. The overall warmer surface of the Baltic Sea in the two-way coupled ICONGETM run causes a predominantly warmer lower troposphere. As a result, the daily-mean 2-m temperature is about $0.5\,\mathrm{K}$ to $2\,\mathrm{K}$ higher (Fig. 8).

Over the upwelling regions, however, where cold deep water has risen to the surface, only the two-way coupled ICONGETM run is able to reproduce the cooling in the $2\,\mathrm{m}$ temperatures of between minus $1\,\mathrm{K}$ to $2\,\mathrm{K}$ against the surroundings. The two-way coupled atmosphere-ocean simulation thus provide a more realistic representation of actual weather conditions. This is also reflected in a better agreement when comparing the model results with air temperature measured onboard the RV Meteor off the island of Gotland during the above-mentioned field campaign. While the temperature is occasionally significantly underestimated by up to $2.5\,\mathrm{K}$ by the uncoupled/one-way coupled ICON simulation, the values from the two-way coupled ICONGETM run are in the same range as the measurements and the temporal development also agrees much better with the observations (Fig. 9), especially after 10 days of simulations.

https://doi.org/10.5194/gmd-2020-269
Preprint. Discussion started: 21 October 2020

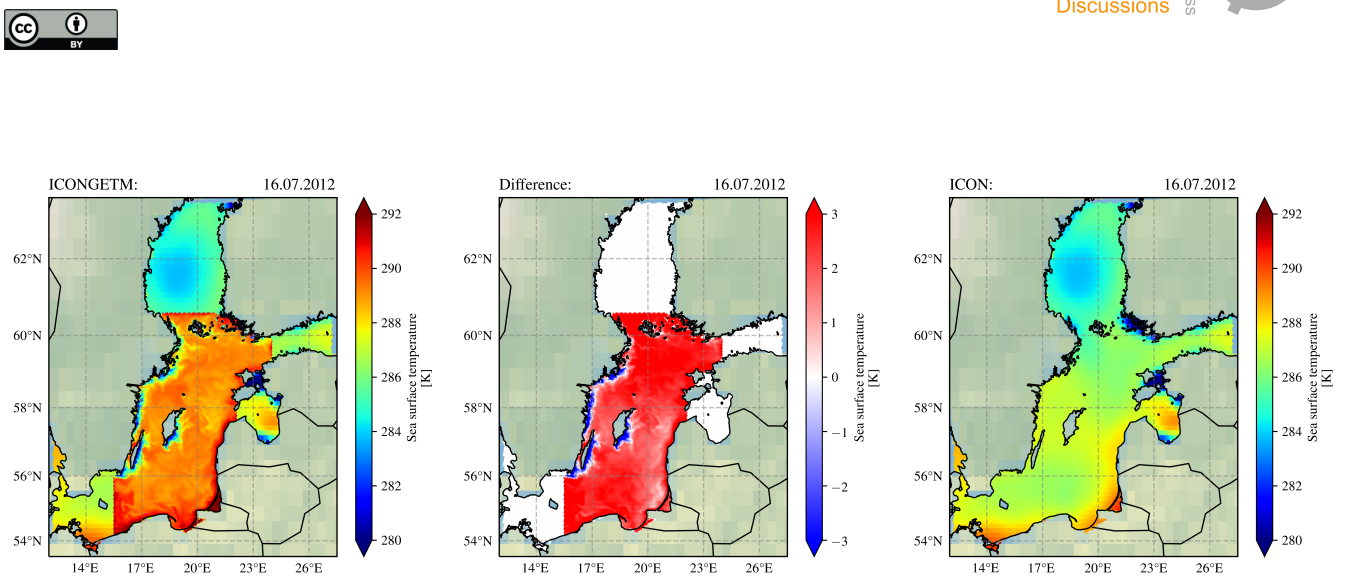

Figure 7. Daily mean sea surface temperature (SST) from the two-way coupled ICONGETM run (left panel), and the uncoupled/one-way coupled ICON run (right panel), as well as the difference (central panel; ICONGETM minus ICON) for 16 July 2012. Outside the domain of simulated SST in the Central Baltic Sea, the two-way coupled ICONGETM run also uses the prescribed ICON-internal SST.

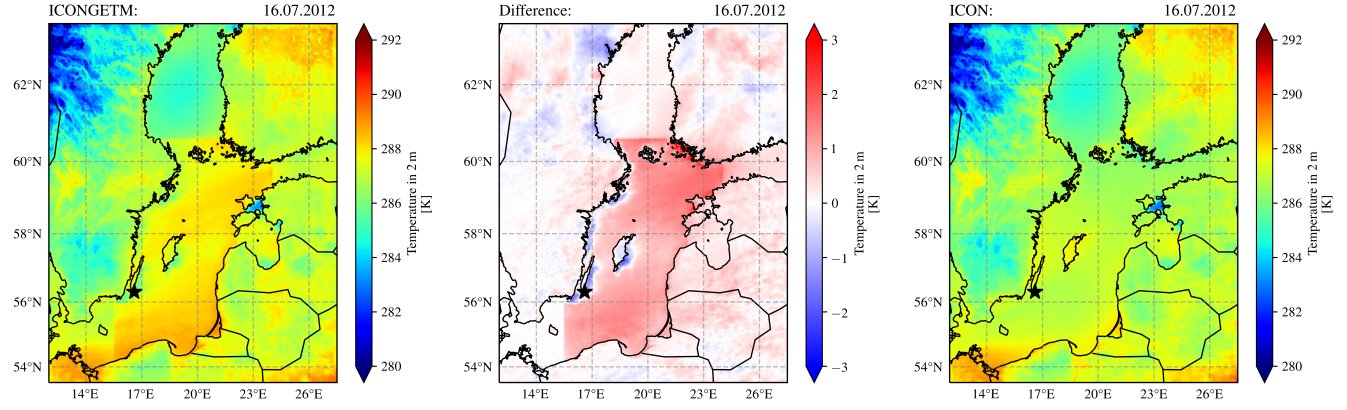

Figure 8. Daily mean 2 m air temperature from the two-way coupled ICONGETM simulation (left panel) and the uncoupled/one-way coupled ICON simulation (right panel), as well as the difference (central panel; ICONGETM minus ICON) for 16 July 2012. The black star south-east of the island of Öland marks the position of the vertical profiles shown in Fig. 12.

The interactive coupling between ICON and GETM also affects the synoptic-scale dynamic meteorology and leads to local effects in the atmospheric boundary layer. The warmer Baltic Sea and higher lower-troposphere temperatures in the two-way coupled ICONGETM simulation result in a mean sea-level pressure that is up to 1 hPa lower over sea and adjacent land than in the uncoupled/one-way coupled ICON run (Fig. 10).

Thus, the low-pressure area over the northern Baltic Sea, which causes the observed upwelling event, is even stronger in the two-way coupled simulation. The resulting higher pressure gradient between the Baltic low and the high over Western Europe (Fig. 10) leads to an increase of the near-surface wind field over a large part of the water surface, while locally wind

https://doi.org/10.5194/gmd-2020-269
Preprint. Discussion started: 21 October 2020

Geoscientific Model Development Discussions
Open Access
EGU

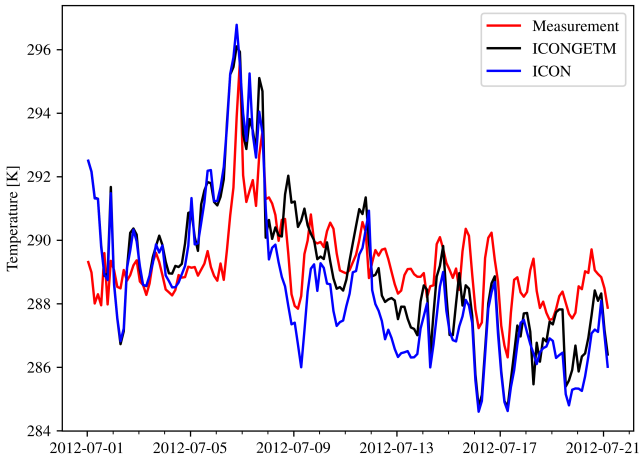

Figure 9. Air temperature in the Eastern Gotland Basin over the period July 1 – 21, 2012. Compared are 3-hourly measurements in 29.1 m onboard the RV Meteor with model results from the two-way coupled ICONGETM and uncoupled/one-way coupled ICON simulations, respectively.

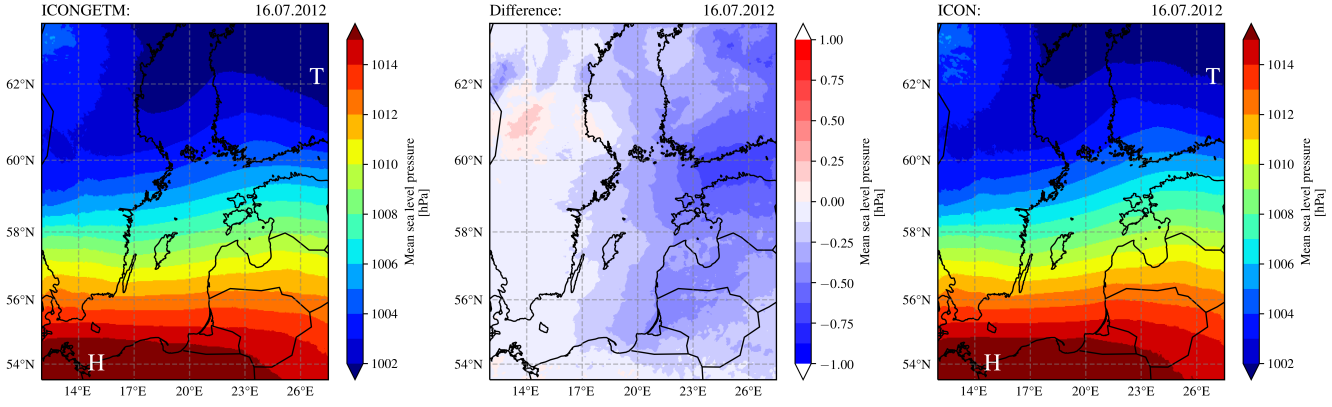

Figure 10. Daily mean sea-level pressure from the two-way coupled ICONGETM simulation (left panel) and the uncoupled/one-way coupled ICON simulation (right panel), as well as the difference (central panel; ICONGETM minus ICON) for 16 July 2012. 'T' and 'H' mark surface lows and highs, respectively.

velocity is reduced in the upwelling regions (Fig. 11). The weather conditions leading to the upwelling event are therefore more pronounced in the two-way coupled model run.

The effects of the interactive atmosphere-ocean coupling on the boundary layer dynamics is most evident for the upwelling regions. Fig. 12 shows vertical profiles of potential temperature and specific humidity over the upwelling area east of Öland. Compared are the profiles for 16 July 2012 at noon and midnight, when the upwelling event was most pronounced in this area. As a result of the upwelling of cold deep water, the potential temperature is reduced by up to 1.5 K to 2 K and atmospheric strat-

https://doi.org/10.5194/gmd-2020-269
Preprint. Discussion started: 21 October 2020

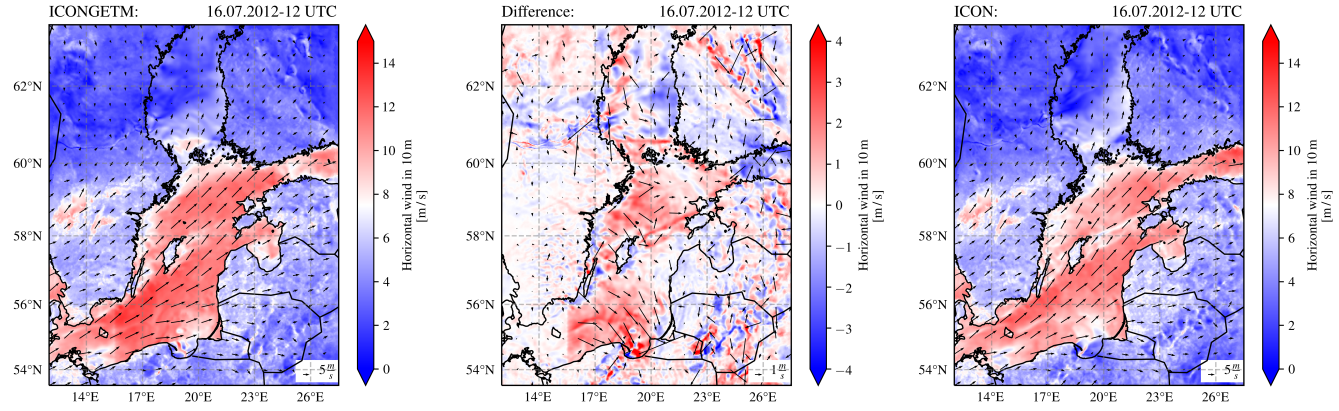

Figure 11. 10 m horizontal wind field from the two-way coupled ICONGETM simluation (left panel) and the uncoupled/one-way coupled ICON simulation (right panel), as well as the difference (central panel; ICONGETM minus ICON) for 16 July 2012 12 UTC. Displayed are the wind vectors (reference vector at the bottom of the figure, units of $\mathrm{m\,s^{-1}}$) and the wind speed (coloured).

ification is increased in the lowermost 50 m to 150 m at noon and mid-night, respectively. The two-way coupled ICONGETM run also shows slightly enhanced gradients in the potential temperature profile at the upper boundary layer. The more stable stratification has an effect on the boundary-layer mixing, whereby humid air is more concentrated in the central to upper part of the boundary layer while it is less in the lowermost part due to reduced evaporation. In addition, there is less momentum mixed downwards (Fig. 12). This is also a likely explanation for the locally reduced wind velocity in the upwelling regions, in addition to the strengthening of the local land-sea circulation (cf. Fig. 11).

4.2.2 Coupling effects in the ocean

In Fig. 13, the sea surface temperature (SST) from all model simulations are compared to satellite data.

Due to the forcing with meteorological reanalysis data, the SST from the uncoupled simulation shows best agreement with the satellite data and most pronounced upwelling activity. The SST from the two-way coupled simulation is only slightly colder, but is clearly overestimated in the one-way coupled simulation. This overestimation results from a continuous increase of near surface temperature, see Fig. 14 for the evolution in the Eastern Gotland Basin.

The evolution indicates that the surface heat flux used in the one-way coupled GETM simulation is overestimated after 12 July 2012. For the one-way coupled simulation, the heat flux provided by ICON is calculated in terms of the too cold ICON-internal SST, see Fig. 7. In the uncoupled and two-way coupled simulations, the surface heat flux is calculated in terms of the SST from GETM, either within GETM or ICON, respectively. Henceforth, the fluxes are adapting more conveniently to the warming ocean. The temperature differences are not only confined to the sea surface, see Fig. 15 for vertical profiles of temperature and salinity in the Eastern Gotland Basin.

In the upper 20 m the temperatures from the uncoupled and two-way coupled simulations are very similar and do excellently agree with the measurements, cf. Fig. 15 B. The temperature from the one-way coupled simulation is approximately 1.5 K too

https://doi.org/10.5194/gmd-2020-269
Preprint. Discussion started: 21 October 2020

Geoscientific Model Development Discussions

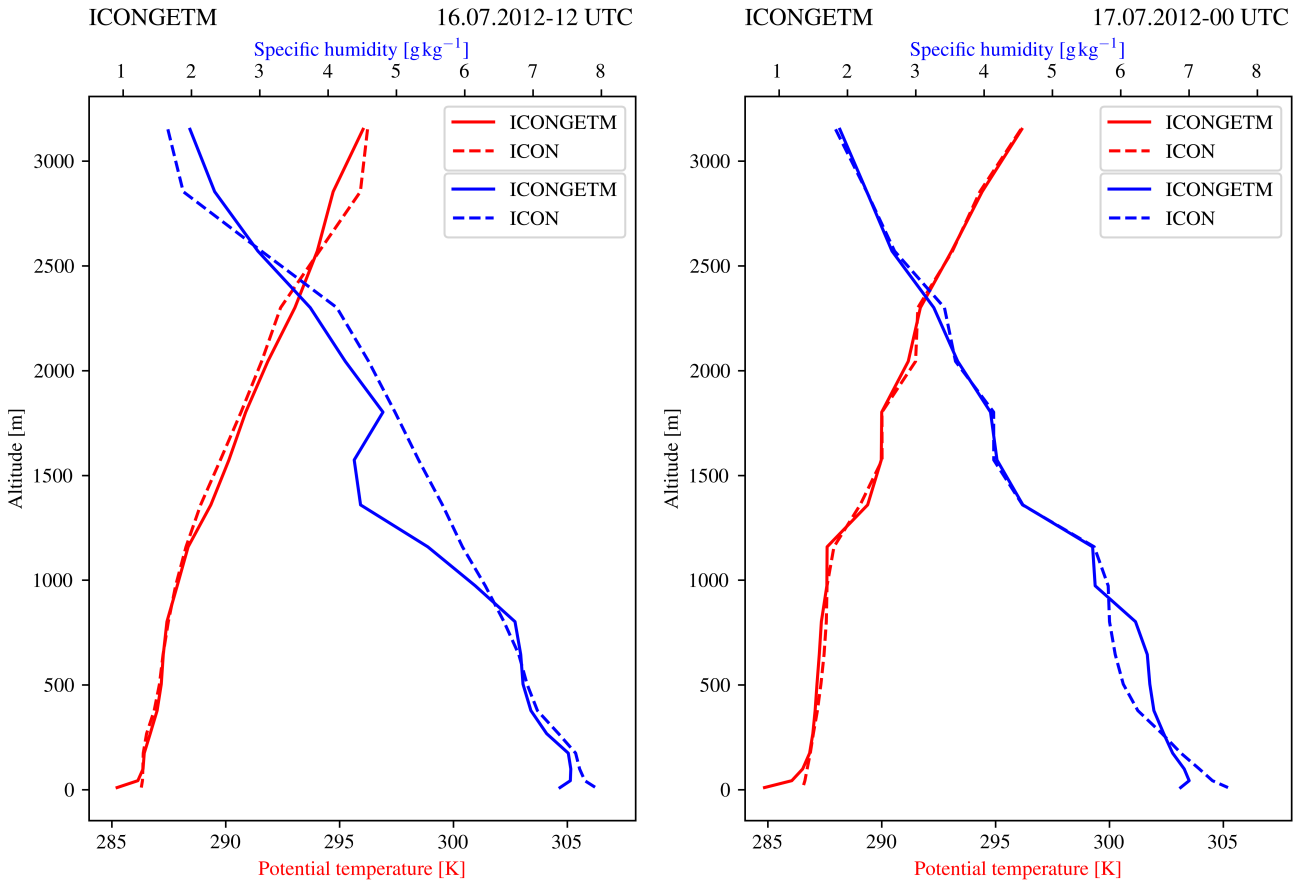

Figure 12. Atmospheric vertical profiles of potential temperature and specific humidity from the two-way coupled ICONGETM run and the uncoupled/one-way coupled ICON run, for 16 (left) and 17 (right) July 2012 at 12 UTC and 00 UTC, respectively. The profiles are obtained south-east of the island of Öland (see black star in Fig. 8).

warm. Within the thermocline ($20-40\,\mathrm{m}$ depth) the temperature profiles do show a stronger difference. When these deviations are compared against the temporal variability of the temperature in an 8 days interval, it becomes clear that the differences can be attributed to the natural variability of the thermocline in the Central Baltic Sea, see Fig. 15 B (for better visibility only the variability of the uncoupled simulation is shown). A slightly different excitation timing of wind driven processes, i.e. near inertial internal waves, are subsequently causing the differences between the analysed profiles.

The salinity differences between the simulations show, in analogy to the temperature, deviations in the thermocline, but are also within the variability observed over an 8 day time period. In contrast to the surface, the deep water below the thermocline is virtually not affected by the different atmospheric forcing. This is caused by the strong density gradients in the thermo- and

https://doi.org/10.5194/gmd-2020-269
Preprint. Discussion started: 21 October 2020

Geoscientific Model Development Discussions
Open Access
EGU

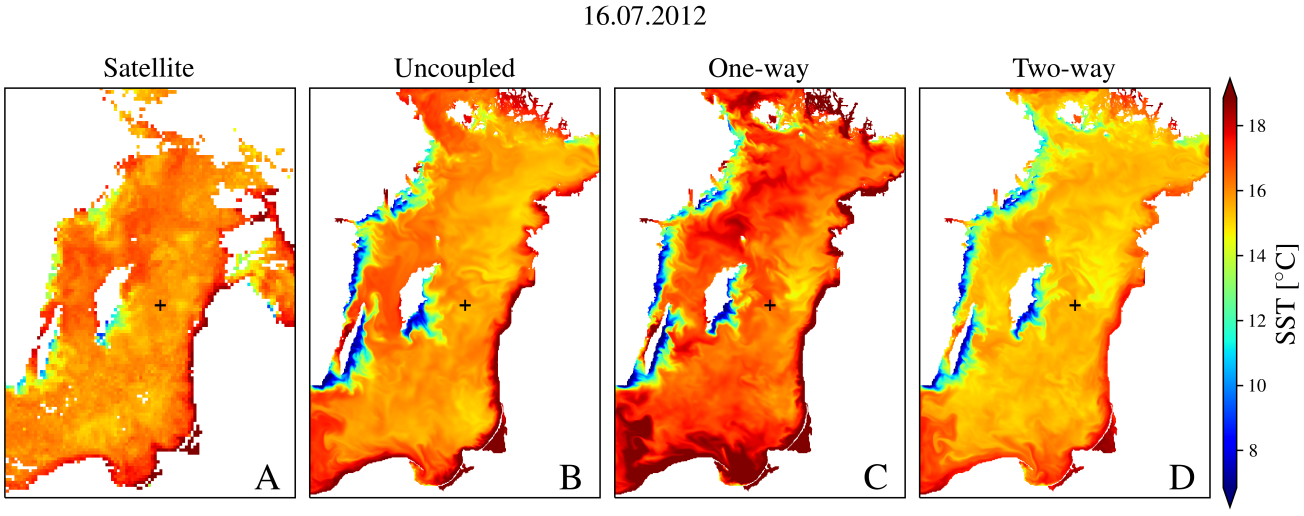

Figure 13. Daily mean sea surface temperature from satellites (A) and simulated by GETM in the uncoupled (B), one-way (C) and two-way (D) coupled simulation for 16 July 2012. The colorbar is identical to Fig. 7. The SST derived from satellite data was provided by the Federal Maritime and Hydrographic Agency of Germany (BSH). The black cross marks the position of station TF271 in the Eastern Gotland Basin.

300 halocline, inhibiting a significant turbulent transport of heat and salt on the timescales analysed by Reissmann et al. (2009); Holtermann et al. (2020).

5 Discussion

The coupled model system ICONGETM supports the exchange of fluxes and state variables across the air-sea interface. The flux calculation in the atmosphere model ICON is very complex and deeply nested in the model code and cannot be switched
305 off by minor changes. Therefore, the fluxes calculated in ICON are exchanged and applied in GETM. For two-way coupled simulations, they are based on the sea surface temperature from GETM. The calculation of fluxes in the ocean model GETM in terms of exchanged atmospheric state variables is not recommended. Applying different fluxes in the atmosphere and ocean would cause energetic inconsistencies in the coupled system.

Ideally, the air-sea fluxes should be calculated in the mediator/coupler component in terms of provided state variables from
310 the atmosphere and ocean. These fluxes can then be applied in the atmosphere and ocean over the same period until new fluxes are provided in the next coupling time step and guarantees energetic consistency. Furthermore, the flux calculation in the mediator is done directly on the high-resolution exchange grid. A central mediator component also offers the most straight-forward extension of the coupled system by other models (e.g. ice model, land surface model). One drawback of the flux calculation outside the single models can be stability issues for explicit time stepping schemes or complex coupling
315 implementations for implicit time stepping schemes.

https://doi.org/10.5194/gmd-2020-269
Preprint. Discussion started: 21 October 2020

Geoscientific Model Development Discussions
Open Access
EGU

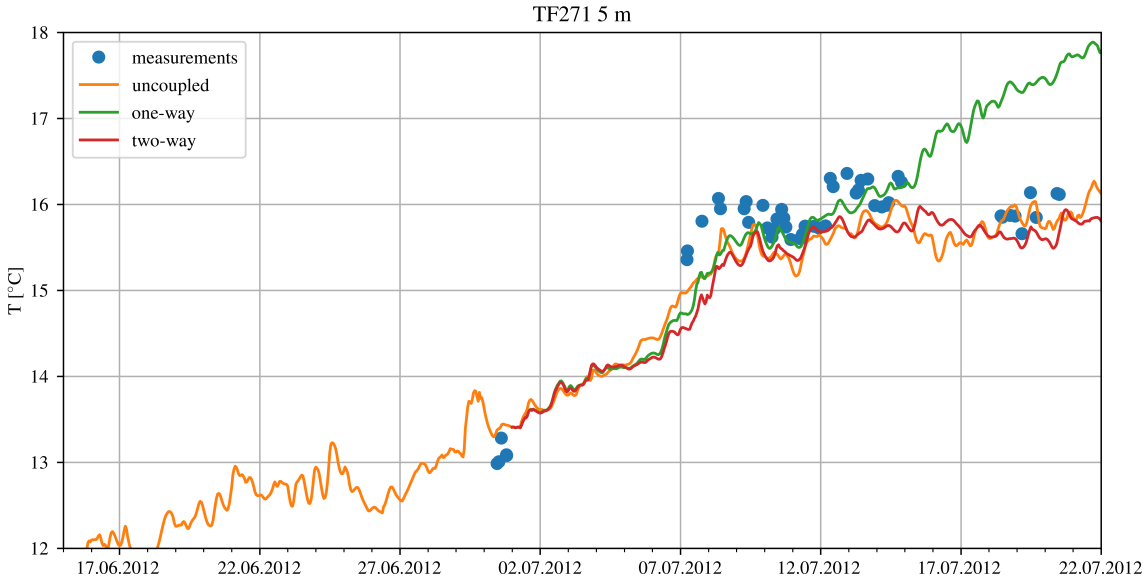

Figure 14. Temperature in 5 m depth at station TF271 from CTD measurements and the three model simulations. The one- and two-way coupled simulations are started at 1 July 2012, after the uncoupled spin-up period.

Due to the nature of the conservative interpolation, small differences such as in the sea surface temperature from ICON and GETM in Fig. 7 and 13, respectively, can occur. Fig. 6 shows the very same effect already for a very academic example. However, conservation over the whole coupling interface is ensured. Additionally, conservation has to be guaranteed for energetic consistency.

The two-way coupled simulation presented in the previous section was conducted with a coupling time step of $3\,\mathrm{min}$ and showed an overhead of approximately $15\,\%$ compared to the uncoupled simulation. The majority is spent for the initialization. This demonstrates the excellent performance of the developed model system based on ESMF/NUOPC and its potential for future high-resolution coupled atmosphere-ocean simulations with fast feedback integration.

6 Conclusions and outlook

The newly developed model ICONGETM combines a conservative flux interpolation between the atmosphere model ICON and the regional ocean model GETM. Furthermore, it uses an exchange grid for the data exchange based on the NUOPC routines provided through the ESMF library. The demonstration example shows that there is now a coupled model available which allows the investigation of processes at the air-sea interface with high-resolved model simulations.

https://doi.org/10.5194/gmd-2020-269
Preprint. Discussion started: 21 October 2020

Geoscientific Model Development Discussions
Open Access
EGU

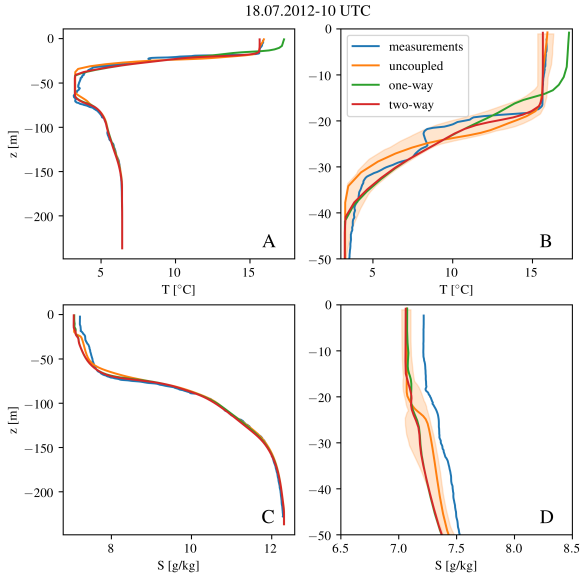

Figure 15. Temperature and salinity profiles at station TF271 from CTD measurements and the three model simulations. Panels A and C depict the whole water column, B and D a zoom towards the sea surface. The light orange shaded area depicts the variability of the uncoupled simulation within an 8 days time interval (14 – 21 July 2012).

Any extension of ICONGETM with other components like sea-ice or wave models etc. is possible with a minimized implementational effort, since only component specific details have to be implemented. Other coupling routines are provided by the NUOPC layer or have been already implemented in the model.

Code availability. The code for ICONGETM v1.0, including the used model codes for ICON and GETM, is permanently available through Zenodo (https://doi.org/10.5281/zenodo.3904461), if a valid ICON license is presented to the authors. The Software License Agreement for ICON from the German Weather Service (DWD) can be found at https://code.mpimet.mpg.de/projects/iconpublic. Access to the code has been granted to the editor for the review process of this paper.

Author contributions. The code has been designed, developed and implemented by TPB in cooperation with KK. The demonstration setup was provided by TPB and BH for ICON and PH and KK for GETM. The coupling configuration has been prepared by TPB and KK and discussed with all authors. BH and TPB evaluated the meteorological results of the simulation, i.e. ICON. PH and KK evaluated the simulation results on the ocean side, i.e. GETM. HR advised and discussed the flux exchange as well as the coupling strategy. OK advised

https://doi.org/10.5194/gmd-2020-269
Preprint. Discussion started: 21 October 2020

the code development and supported the implementation of mathematical utility routines. All authors contributed to this paper in the sections corresponding to their part during the work flow.

Competing interests. The authors declare having no conflict of interest.

Acknowledgements. The authors like to acknowledge the contributions by the ESMF support, namely Fei Lui, Robert Oehmke and Gerhard Theurich. They have replied to every support request and improved the ESMF library during the development of the model code.
This work is the outcome of the model coupling initiative LOCUS (Land-ocean interaction mediated by coastal upwelling and sea breeze) funded by the Leibniz institutes TROPOS and IOW.
The authors gratefully acknowledge additional financial support by the German Research Foundation for the Collaborative Research Center TRR181 on Energy Transfers in Atmosphere and Ocean (Project 274762653) and the funding of Peter Holtermann by grant HO 5891/1-1, as well as the project MOSSCO (Modular System for Shelves and Coasts; FKZ 03F0740B, funded by the German Federal Ministry of Research and Education).

https://doi.org/10.5194/gmd-2020-269
Preprint. Discussion started: 21 October 2020

References

Aldrian, E., Sein, D., Jacob, D., Gates, L. D., and Podzun, R.: Modelling Indonesian rainfall with a coupled regional model, Clim. Dyn., 25, 1–17, https://doi.org/10.1007/s00382-004-0483-0, http://link.springer.com/10.1007/s00382-004-0483-0, 2005.

Badin, G., Tandon, A., and Mahadevan, A.: Lateral Mixing in the Pycnocline by Baroclinic Mixed Layer Eddies, J. Phys. Oceanogr., 41, 2080–2101, https://doi.org/10.1175/JPO-D-11-05.1, http://journals.ametsoc.org/doi/10.1175/JPO-D-11-05.1, 2011.

Balaji, V., Anderson, J., Held, I., Winton, M., Durachta, J., Malyshev, S., and Stouffer, R. J.: The Exchange Grid: A mechanism for data exchange between Earth System components on independent grids, in: Parallel Comput. Fluid Dyn. 2005, pp. 179–186, Elsevier, https://doi.org/10.1016/B978-044452206-1/50021-5, https://linkinghub.elsevier.com/retrieve/pii/B9780444522061500215, 2006.

Bechtold, P., Köhler, M., Jung, T., Doblas-Reyes, F., Leutbecher, M., Rodwell, M. J., Vitart, F., and Balsamo, G.: Advances in simulating atmospheric variability with the ECMWF model: From synoptic to decadal time-scales, Q. J. R. Meteorol. Soc., 134, 1337–1351, https://doi.org/10.1002/qj.289, http://doi.wiley.com/10.1002/qj.289, 2008.

Borchert, S., Zhou, G., Baldauf, M., Schmidt, H., Zängl, G., and Reinert, D.: The upper-atmosphere extension of the ICON general circulation model, Geosci. Model Dev. Discuss., m, 1–50, https://doi.org/10.5194/gmd-2018-289, https://www.geosci-model-dev-discuss.net/gmd-2018-289/, 2018.

Burchard, H. and Bolding, K.: GETM – a General Estuarine Transport Model. Scientific Documentation, Tech. rep., European Commission, http://publications.jrc.ec.europa.eu/repository/handle/JRC23237http://publications.jrc.ec.europa.eu/repository/bitstream/JRC23237/EUR20253EN.pdf, 2002.

Christensen, J. H., Larsen, M. A. D., Christensen, O. B., Drews, M., and Stendel, M.: Robustness of European climate projections from dynamical downscaling, Clim. Dyn., 53, 4857–4869, https://doi.org/10.1007/s00382-019-04831-z, http://link.springer.com/10.1007/s00382-019-04831-z, 2019.

Chrysagi, E., Holtermann, P. L., Umlauf, L., Klingbeil, K., and Burchard, H.: High-resolution simulations of submesoscale processes in the Baltic Sea: The role of storm events, J. Geophys. Res. Ocean., https://doi.org/10.1029/2020JC016411, 2020.

Clark, P., Roberts, N., Lean, H., Ballard, S. P., and Charlton-Perez, C.: Convection-permitting models: a step-change in rainfall forecasting, Meteorol. Appl., 23, 165–181, https://doi.org/10.1002/met.1538, http://doi.wiley.com/10.1002/met.1538, 2016.

Crueger, T., Giorgetta, M. A., Brokopf, R., Esch, M., Fiedler, S., Hohenegger, C., Kornblueh, L., Mauritsen, T., Nam, C., Naumann, A. K., Peters, K., Rast, S., Roeckner, E., Sakradzija, M., Schmidt, H., Vial, J., Vogel, R., and Stevens, B.: ICON-A, The Atmosphere Component of the ICON Earth System Model: II. Model Evaluation, J. Adv. Model. Earth Syst., 10, 1638–1662, https://doi.org/10.1029/2017MS001233, http://doi.wiley.com/10.1029/2017MS001233, 2018.

Dickinson, R. E., Errico, R. M., Giorgi, F., and Bates, G. T.: A regional climate model for the western United States, Clim. Change, 15, https://doi.org/10.1007/BF00240465, http://link.springer.com/10.1007/BF00240465, 1989.

Dipankar, A., Stevens, B., Heinze, R., Moseley, C., Zängl, G., Giorgetta, M. A., and Brdar, S.: Large eddy simulation using the general circulation model ICON, J. Adv. Model. Earth Syst., 7, 963–986, https://doi.org/10.1002/2015MS000431, http://doi.wiley.com/10.1002/2015MS000431, 2015.

Doms, G., Förstner, J., Heise, E., Herzog, H.-J., Mironov, D., Raschendorfer, M., Reinhardt, T., Ritter, B., Schrodin, R., Schulz, J.-P., and Vogel, G.: A description of the Nonhydrostatic Regional COSMOS Model, Part II: Physical parameterization, Tech. rep., Deutscher Wetterdienst, Offenbach, http://www.cosmo-model.org, 2011.

https://doi.org/10.5194/gmd-2020-269
Preprint. Discussion started: 21 October 2020

Donlon, C. J., Martin, M., Stark, J., Roberts-Jones, J., Fiedler, E., and Wimmer, W.: The Operational Sea Surface Temperature and Sea Ice Analysis (OSTIA) system, Remote Sens. Environ., 116, 140–158, https://doi.org/10.1016/j.rse.2010.10.017, https://linkinghub.elsevier.com/retrieve/pii/S0034425711002197, 2012.

DWD: Weather Forecast System, https://www.dwd.de/EN/research/weatherforecasting/num_modelling/01_num_weather_prediction_modells/icon_description.html, 2019.

Fennel, W., Seifert, T., and Kayser, B.: Rossby radii and phase speeds in the Baltic Sea, Cont. Shelf Res., 11, 23–36, https://doi.org/10.1016/0278-4343(91)90032-2, https://linkinghub.elsevier.com/retrieve/pii/0278434391900322, 1991.

Fennel, W., Radtke, H., Schmidt, M., and Neumann, T.: Transient upwelling in the central Baltic Sea, Cont. Shelf Res., 30, 2015–2026, https://doi.org/10.1016/j.csr.2010.10.002, https://linkinghub.elsevier.com/retrieve/pii/S0278434310003092, 2010.

Giorgetta, M. A., Brokopf, R., Crueger, T., Esch, M., Fiedler, S., Helmert, J., Hohenegger, C., Kornblueh, L., Köhler, M., Manzini, E., Mauritsen, T., Nam, C., Raddatz, T., Rast, S., Reinert, D., Sakradzija, M., Schmidt, H., Schneck, R., Schnur, R., Silvers, L., Wan, H., Zängl, G., and Stevens, B.: ICON-A, the Atmosphere Component of the ICON Earth System Model: I. Model Description, J. Adv. Model. Earth Syst., 10, 1613–1637, https://doi.org/10.1029/2017MS001242, http://doi.wiley.com/10.1029/2017MS001242, 2018.

Gräwe, U., Holtermann, P. L., Klingbeil, K., and Burchard, H.: Advantages of vertically adaptive coordinates in numerical models of stratified shelf seas, Ocean Model., 92, 56–68, https://doi.org/10.1016/j.ocemod.2015.05.008, http://linkinghub.elsevier.com/retrieve/pii/S1463500315000979, 2015.

Gräwe, U., Klingbeil, K., Kelln, J., and Dangendorf, S.: Decomposing Mean Sea Level Rise in a Semi-Enclosed Basin, the Baltic Sea, J. Clim., 32, 3089–3108, https://doi.org/10.1175/JCLI-D-18-0174.1, http://journals.ametsoc.org/doi/10.1175/JCLI-D-18-0174.1, 2019.

Gröger, M., Arneborg, L., Dieterich, C., Höglund, A., and Meier, H. E. M.: Summer hydrographic changes in the Baltic Sea, Kattegat and Skagerrak projected in an ensemble of climate scenarios downscaled with a coupled regional ocean–sea ice–atmosphere model, Clim. Dyn., 53, 5945–5966, https://doi.org/10.1007/s00382-019-04908-9, http://link.springer.com/10.1007/s00382-019-04908-9, 2019.

Gustafsson, N., Nyberg, L., and Omstedt, A.: Coupling of a High-Resolution Atmospheric Model and an Ocean Model for the Baltic Sea, Mon. Weather Rev., 126, 2822–2846, https://doi.org/10.1175/1520-0493(1998)126<2822:COAHRA>2.0.CO;2, http://journals.ametsoc.org/doi/abs/10.1175/1520-0493%281998%29126%3C2822%3ACOAHRA%3E2.0.CO%3B2, 1998.

Hanke, M., Redler, R., Holfeld, T., and Yastremsky, M.: YAC 1.2.0: New aspects for coupling software in Earth system modelling, Geosci. Model Dev., 9, 2755–2769, https://doi.org/10.5194/gmd-9-2755-2016, 2016.

Heinze, R., Dipankar, A., Henken, C. C., Moseley, C., Sourdeval, O., Trömel, S., Xie, X., Adamidis, P., Ament, F., Baars, H., Barthlott, C., Behrendt, A., Blahak, U., Bley, S., Brdar, S., Brueck, M., Crewell, S., Deneke, H., Di Girolamo, P., Evaristo, R., Fischer, J., Frank, C., Friederichs, P., Göcke, T., Gorges, K., Hande, L., Hanke, M., Hansen, A., Hege, H.-c., Hoose, C., Jahns, T., Kalthoff, N., Klocke, D., Kneifel, S., Knippertz, P., Kuhn, A., van Laar, T., Macke, A., Maurer, V., Mayer, B., Meyer, C. I., Muppa, S. K., Neggers, R. A. J., Orlandi, E., Pantillon, F., Pospichal, B., Röber, N., Scheck, L., Seifert, A., Seifert, P., Senf, F., Siligam, P., Simmer, C., Steinke, S., Stevens, B., Wapler, K., Weniger, M., Wulfmeyer, V., Zängl, G., Zhang, D., and Quaas, J.: Large-eddy simulations over Germany using ICON: a comprehensive evaluation, Q. J. R. Meteorol. Soc., 143, 69–100, https://doi.org/10.1002/qj.2947, http://doi.wiley.com/10.1002/qj.2947, 2017.

Hill, C., DeLuca, C., Balaji, V., Suarez, M., and Da Silva, A. M.: The architecture of the earth system modeling framework, Comput. Sci. Eng., 6, 18–28, https://doi.org/10.1109/MCISE.2004.1255817, http://ieeexplore.ieee.org/document/1255817/, 2004.

Hofmeister, R., Burchard, H., and Beckers, J.-M.: Non-uniform adaptive vertical grids for 3D numerical ocean models, Ocean Model., 33, 70–86, https://doi.org/10.1016/j.ocemod.2009.12.003, https://linkinghub.elsevier.com/retrieve/pii/S1463500309002248, 2010.

https://doi.org/10.5194/gmd-2020-269
Preprint. Discussion started: 21 October 2020

Holtermann, P., Prien, R., Naumann, M., and Umlauf, L.: Interleaving of oxygenized intrusions into the Baltic Sea redoxcline, Limnol. Oceanogr., 65, 482–503, https://doi.org/10.1002/lno.11317, https://onlinelibrary.wiley.com/doi/abs/10.1002/lno.11317, 2020.

Holtermann, P. L., Burchard, H., Gräwe, U., Klingbeil, K., and Umlauf, L.: Deep-water dynamics and boundary mixing in a nontidal stratified basin: A modeling study of the Baltic Sea, J. Geophys. Res. Ocean., 119, 1465–1487, https://doi.org/10.1002/2013JC009483, http://doi.wiley.com/10.1002/2013JC009483, 2014.

Klingbeil, K. and Burchard, H.: Implementation of a direct nonhydrostatic pressure gradient discretisation into a layered ocean model, Ocean Model., 65, 64–77, https://doi.org/10.1016/j.ocemod.2013.02.002, http://dx.doi.org/10.1016/j.ocemod.2013.02.002, 2013.

Klingbeil, K., Mohammadi-Aragh, M., Gräwe, U., and Burchard, H.: Quantification of spurious dissipation and mixing – Discrete variance decay in a Finite-Volume framework, Ocean Model., 81, 49–64, https://doi.org/10.1016/j.ocemod.2014.06.001, https://linkinghub.elsevier.com/retrieve/pii/S1463500314000754, 2014.

Klingbeil, K., Lemarié, F., Debreu, L., and Burchard, H.: The numerics of hydrostatic structured-grid coastal ocean models: State of the art and future perspectives, Ocean Model., 125, 80–105, https://doi.org/10.1016/j.ocemod.2018.01.007, http://linkinghub.elsevier.com/retrieve/pii/S1463500318300180, 2018.

Kondo, J.: Air-sea bulk transfer coefficients in diabatic conditions, Boundary-Layer Meteorol., 9, 91–112, https://doi.org/10.1007/BF00232256, 1975.

Lange, X., Burchard, H., and Klingbeil, K.: Inversions of estuarine circulation are frequent in a weakly tidal estuary with variable wind forcing and seaward salinity fluctuations, J. Geophys. Res. Ocean., https://doi.org/10.1029/2019JC015789, 2020.

Laprise, R.: Regional climate modelling, J. Comput. Phys., 227, 3641–3666, https://doi.org/10.1016/j.jcp.2006.10.024, https://linkinghub.elsevier.com/retrieve/pii/S0021999106005407, 2008.

Lemmen, C., Hofmeister, R., Klingbeil, K., Nasermoaddeli, M. H., Kerimoglu, O., Burchard, H., Kösters, F., and Wirtz, K. W.: Modular System for Shelves and Coasts (MOSSCO v1.0) – a flexible and multi-component framework for coupled coastal ocean ecosystem modelling, Geosci. Model Dev., 11, 915–935, https://doi.org/10.5194/gmd-11-915-2018, https://www.geosci-model-dev.net/11/915/2018/, 2018.

Linardakis, L., Reinert, D., and Gassmann, A.: ICON Grid Documentation, Tech. rep., DKRZ, Hamburg, https://www.dkrz.de/SciVis/hd-cp-2/en-icon_grid.pdf?lang=en, 2011.

Miller, N. L. and Kim, J.: Numerical Prediction of Precipitation and River Flow over the Russian River Watershed during the January 1995 California Storms, Bull. Am. Meteorol. Soc., 77, 101–105, https://doi.org/10.1175/1520-0477(1996)077<0101:NPOPAR>2.0.CO;2, http://journals.ametsoc.org/doi/abs/10.1175/1520-0477%281996%29077%3C0101%3ANPOPAR%3E2.0.CO%3B2, 1996.

Mlawer, E. J., Taubman, S. J., Brown, P. D., Iacono, M. J., and Clough, S. A.: Radiative transfer for inhomogeneous atmospheres: RRTM, a validated correlated-k model for the longwave, J. Geophys. Res. Atmos., 102, 16 663–16 682, https://doi.org/10.1029/97JD00237, http://doi.wiley.com/10.1029/97JD00237, 1997.

Purr, C., Brisson, E., and Ahrens, B.: Convective Shower Characteristics Simulated with the Convection-Permitting Climate Model COSMO-CLM, Atmosphere (Basel)., 10, 810, https://doi.org/10.3390/atmos10120810, https://www.mdpi.com/2073-4433/10/12/810, 2019.

Reinert, D., Prill, F., Frank, H., Denhard, M., and Zängl, G.: Database Reference Manual for ICON and ICON-EPS, Tech. rep., DWD, Offenbach, https://doi.org/10.5676/DWD_pub/nwv/icon_1.2.12, https://www.dwd.de/DWD/forschung/nwv/fepub/icon_database_main.pdf, 2020.

Reissmann, J. H., Burchard, H., Feistel, R., Hagen, E., Lass, H. U., Mohrholz, V., Nausch, G., Umlauf, L., and Wieczorek, G.: Vertical mixing in the Baltic Sea and consequences for eutrophication – A review, Prog. Oceanogr., 82, 47–80, https://doi.org/10.1016/j.pocean.2007.10.004, https://linkinghub.elsevier.com/retrieve/pii/S0079661109000159, 2009.

https://doi.org/10.5194/gmd-2020-269
Preprint. Discussion started: 21 October 2020

Ren, X. and Qian, Y.: A coupled regional air-sea model, its performance and climate drift in simulation of the East Asian summer monsoon in 1998, Int. J. Climatol., 25, 679–692, https://doi.org/10.1002/joc.1137, http://doi.wiley.com/10.1002/joc.1137, 2005.

Rummukainen, M., Räisänen, J., Bringfelt, B., Ullerstig, A., Omstedt, A., Willén, U., Hansson, U., and Jones, C.: A regional climate model for northern Europe: Model description and results from the downscaling of two GCM control simulations, Clim. Dyn., 17, 339–359, https://doi.org/10.1007/s003820000109, 2001.

Saha, S., Moorthi, S., Wu, X., Wang, J., Nadiga, S., Tripp, P., Behringer, D., Hou, Y.-T., Chuang, H.-y., Iredell, M., Ek, M., Meng, J., Yang, R., Mendez, M. P., van den Dool, H., Zhang, Q., Wang, W., Chen, M., and Becker, E.: The NCEP Climate Forecast System Version 2, J. Clim., 27, 2185–2208, https://doi.org/10.1175/JCLI-D-12-00823.1, http://journals.ametsoc.org/doi/10.1175/JCLI-D-12-00823.1, 2014.

Schrum, C.: Regional Climate Modeling and Air-Sea Coupling, in: Oxford Res. Encycl. Clim. Sci., Oxford University Press, https://doi.org/10.1093/acrefore/9780190228620.013.3, http://climatescience.oxfordre.com/view/10.1093/acrefore/9780190228620.001.0001/acrefore-9780190228620-e-3, 2017.

Schrum, C., Hübner, U., Jacob, D., and Podzun, R.: A coupled atmosphere/ice/ocean model for the North Sea and the Baltic Sea, Clim. Dyn., 21, 131–151, https://doi.org/10.1007/s00382-003-0322-8, 2003.

Seo, H., Miller, A. J., and Roads, J. O.: The Scripps Coupled Ocean–Atmosphere Regional (SCOAR) Model, with Applications in the Eastern Pacific Sector, J. Clim., 20, 381–402, https://doi.org/10.1175/JCLI4016.1, https://journals.ametsoc.org/jcli/article/20/3/381/31767/The-Scripps-Coupled-OceanAtmosphere-Regional-SCOAR, 2007.

Theurich, G., DeLuca, C., Campbell, T., Liu, F., Saint, K., Vertenstein, M., Chen, J., Oehmke, R., Doyle, J., Whitcomb, T., Wallcraft, A., Iredell, M., Black, T., Da Silva, A. M., Clune, T., Ferraro, R., Li, P., Kelley, M., Aleinov, I., Balaji, V., Zadeh, N., Jacob, R., Kirtman, B., Giraldo, F., McCarren, D., Sandgathe, S., Peckham, S., and Dunlap, R.: The earth system prediction suite: Toward a coordinated U.S. modeling capability, Bull. Am. Meteorol. Soc., 97, 1229–1247, https://doi.org/10.1175/BAMS-D-14-00164.1, 2016.

Ullrich, P. A., Jablonowski, C., Kent, J., Lauritzen, P. H., Nair, R., Reed, K. A., Zarzycki, C. M., Hall, D. M., Dazlich, D., Heikes, R., Konor, C., Randall, D., Dubos, T., Meurdesoif, Y., Chen, X., Harris, L., Kühnlein, C., Lee, V., Qaddouri, A., Girard, C., Giorgetta, M. A., Reinert, D., Klemp, J., Park, S.-H., Skamarock, W. C., Miura, H., Ohno, T., Yoshida, R., Walko, R., Reinecke, A., and Viner, K.: DCMIP2016: a review of non-hydrostatic dynamical core design and intercomparison of participating models, Geosci. Model Dev., 10, 4477–4509, https://doi.org/10.5194/gmd-10-4477-2017, https://www.geosci-model-dev.net/10/4477/2017/, 2017.

Valcke, S.: The OASIS3 coupler: a European climate modelling community software, Geosci. Model Dev. Discuss., 5, 2139–2178, https://doi.org/10.5194/gmdd-5-2139-2012, 2013.

Woodward, J. R., Pitchford, J. W., and Bees, M. A.: Physical flow effects can dictate plankton population dynamics, J. R. Soc. Interface, 16, 20190 247, https://doi.org/10.1098/rsif.2019.0247, https://royalsocietypublishing.org/doi/10.1098/rsif.2019.0247, 2019.

Zängl, G., Reinert, D., Rípodas, P., and Baldauf, M.: The ICON (ICOsahedral Non-hydrostatic) modelling framework of DWD and MPI-M: Description of the non-hydrostatic dynamical core, Q. J. R. Meteorol. Soc., 141, 563–579, https://doi.org/10.1002/qj.2378, http://doi.wiley.com/10.1002/qj.2378, 2015.